tvst

Lacrimal Apparatus, Eyelids, Orbit

What Is the Best Candidate to Replace the Tarsus? A Biomechanical, Histological, and Optical Study Comparing Five Grafts

Ken Martini[1], Sebastien Schaub[2], Corine Bertoloto[3], Stephanie Baillif[1], Sandra Lassalle[4], Paul Martel[5], and Arnaud Martel[1]

[1] Ophthalmology Department, University Hospital of Nice, Nice, France
[2] Sorbonne University, CNRS, Developmental Biology Laboratory (LBDV), Villefranche-sur-Mer Cedex, France
[3] Mediterranean Center of Molecular Medicine, Nice, France
[4] Laboratory of Clinical and Experimental Pathology, Côte d'Azur University, FHU OncoAge, Pasteur Hospital, Nice, France
[5] Sterlab Laboratory, Vallauris, France

Correspondence: Arnaud Martel, Ophthalmology Department, University Hospital of Nice, 30 Voie Romaine, 06000 Nice, France. e-mail: martel.a@chu-nice.fr

Received: June 17, 2021
Accepted: April 17, 2022
Published: December 6, 2022

Keywords: posterior lamella graft; tarsus; Young's modulus; multi-photonic microscopy; elastin

Citation: Martini K, Schaub S, Bertoloto C, Baillif S, Lassalle S, Martel P, Martel A. What is the best candidate to replace the tarsus? A biomechanical, histological, and optical study comparing five grafts. Transl Vis Sci Technol. 2022;11(12):6, https://doi.org/10.1167/tvst.11.12.6

Purpose: Reconstruction of the posterior lamella after eyelid tumor removal is challenging and not consensual. Tarsus is the most suitable graft, but is only available in small amounts. Herein, we aim to determine the most appropriate way to replace the tarsus by comparing the biomechanical, histological, and optical properties of five commonly used grafts.

Methods: This study was conducted at the University hospital of Nice between June 2019 and June 2020. Five posterior lamella grafts (tarsus, conchal cartilage, sclera, hard palate, and dermis) were harvested in five fresh frozen cadavers. Biomechanical properties were assessed by tractometry. Collagen and elastin fibers were analyzed by using histological analysis and optical characterization with the second harmonic generation imaging.

Results: The mean Young's modulus was 8.92 MPa (range, 2.90–22.90 MPa), 1.05 MPa (range, 0.39–1.76 MPa), 8.72 MPa (range, 2.0–23.50 MPa), 2.57 MPa (range, 0.41–4.35 MPa), and 1.44 MPa (range, 0.71–2.30 MPa) for the tarsus, the conchal cartilage, the sclera, the hard palate mucosa, and the dermis, respectively. The mean tensile strength was 3 MPa (range, 1.70–6.88 MPa), 0.54 MPa (range, 0.13–0.79 MPa), 2.87 MPa (range, 1.23–5.40 MPa), 1.4 MPa (range, 0.21–2.40 MPa) and 1.0 MPa (range, 0.46–1.43 MPa) for the tarsus, the conchal cartilage, the sclera, the hard palate mucosa, and the dermis, respectively. Hard palate mucosa was the closest to the tarsus regarding the ratio of elastin and collagen fibers. The average second harmonic generation intensity was 221 arbitrary units (a.u.) (range, 165–362 a.u.), 182 a.u. (range, 35–259 a.u.), 369 a.u. (range, 206–533 a.u.), 108 a.u. (range, 34–208 a.u.), and 244 a.u. (range, 195–388 a.u.) for the tarsus, the conchal cartilage, the sclera, the hard palate mucosa, and the dermis, respectively. The hard palate mucosa and the dermis were the closest to the tarsus regarding the collagen fiber size and orientation, respectively.

Conclusions: By attributing 2 points for each characteristic (biomechanical, histological, and optical), the hard palate mucosa and the sclera seem to be the most suitable grafts to replace the tarsus.

Translational Relevance: The aim of this article was to assess the biomechanical, histological and optical characteristics of five of the most commonly used tarsal grafts; this may be helpful in decisions for clinical practice.

translational vision science & technology

Introduction

Both upper and lower eyelids can be divided into anterior, middle, and posterior lamella. The anterior lamella comprises the skin and the orbicularis muscle, the middle lamella comprises the retractors, and the posterior lamella comprises the tarsus and the conjunctiva.[1] The tarsus is a fibrocartilaginous plate measuring approximately 25 mm in length by 4 to 10 mm in height.[2] It is made of type I and type III collagen fibers, elastin as well as structural molecule such as aggrecan, cartilage oligomeric matrix proteins, glycosaminoglycans, and proteoglycans.[2] The tarsus also contains the Meibomian glands, which help to stabilize the lacrimal film against evaporation. All these intrinsic characteristics make the tarsus unique. Reconstructing the posterior lamella is mainly mandatory for tumoral defects or lid lengthening.[1,3–5] Not surprisingly, the tarsus itself harvested in the ipsilateral or contralateral eyelid is the gold standard for reconstructing the posterior lamella. However, the tarsus is available in small amounts and its harvest may be associated with eyelid malpositions.[6] Other posterior lamella grafts have been used in the literature, such as the auricular or conchal cartilage, the hard palate mucosa, the donor sclera, the autologous or artificial dermis, and the nasal septal cartilage. Of them, the hard palate mucosa is often considered as the most suitable graft,[7–10] even if complications of the harvested site (e.g., buccal pain and hemorrhage) limit its use.[1] Therefore, the ideal posterior lamella graft for replacing the tarsus is still debated in the literature.[7–9,11,12] The ideal posterior lamella graft should share the tarsus' characteristics: elasticity, rigidity, regular surface, mucosal face, and lipidic secretions. To date, biomechanical and molecular studies comparing the most commonly used posterior lamellar grafts are lacking. The aim of this study was to compare the biomechanical and molecular features of five different posterior lamella grafts to determine which one is the most suitable to replace the tarsus.

Materials and Methods

Tissue Harvesting

This study was conducted at the University Hospital of Nice between June 2019 and June 2020. This study was in accordance with the principles outlined by the declaration of Helsinki and its further amendments. We dissected bilaterally in a full thickness fashion the tarsus, the preauricular dermis, the conchal cartilage, the hard palate mucosa, and the sclera (Fig. 1). The specimen were then cut into 10-mm-wide pieces. The grafts were harvested in five fresh frozen cadavers (one man, four women) with a mean age of 78.2 years (range, 55–91 years). All the cadavers supplied by our laboratory were frozen for 1 to 15 days. The tarsus was harvested through a lid crease incision and separated from the underlying conjunctiva. Autologous dermis graft was harvested in the preauricular area after removal of the epidermis layer with a 15 blade. Conchal cartilage was harvested through an anterior approach without its underlying perichondrium. The sclera was harvested in a four-petals eviscerated globe. We harvested the anterior one-half of the sclera in this study. Hard palate mucosa was harvested in the paramedian region with its underlying periosteum. Biomechanical analyses were carried out in fresh samples within 4 hours after the dissection, whereas histological and optical properties were assessed few days later after having fixed the tissues in formaldehyde 4%.

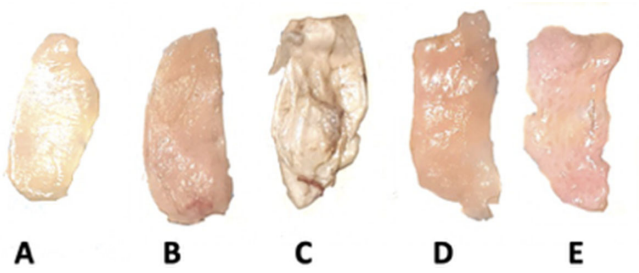

Figure 1. Presentation of the five grafts harvested in our study. (**A**) Tarsus. (**B**) Conchal cartilage. (**C**) Sclera. (**D**) Hard palate. (**E**) Dermis.

Biomechanical Assessment by Tractometry

Fresh samples were analysed by using a tractometer (Adamel Lhomargi, Roissy-en-Brie, France). Each sample was attached and secured with two opposing jaws. A preload was applied to place the tissue in tension. Then, the tension started with a speed of 10 mm/min until obtaining the tissular elongation breakdown. For each graft, we calculated the Young's Modulus as well as the tensile strength. Young's Modulus calculation was as follows:

$\sigma = E\,\varepsilon$, where:
σ is the tensile stress (Pa = N/m^2)
E is the Young's modulus (Pa = N/m^2)
$\varepsilon = (\ell - \ell_0)/\ell_0$ is the proportional deformation

Collagen and Elastin Fiber Histopathology Assessment

Fixed samples were sent to the Pathology Department of the University Hospital of Nice.

Serial sections of paraffin-embedded tissue were cut at 3 μm thickness using a microtome and mounted on microscope slides before being stained for hematoxylin eosin Safran and Verhoeff staining (Benchmark Special Stains automated staining instrument; Ventana Medical Systems, Tucson, AZ). Collagen amount was evaluated on hematoxylin eosin Safran slides and elastin fibers with the Verhoeff staining. Evaluation of the elastin to collagen fiber ratio was established by a senior pathologist (SL).

Microscopic Collagen Fiber Organization Assessment

We analyzed the collagenic structure of each sample by using a multi-photonic microscope on MICA (Microscopie et Imagerie Côte d'Azur) multisite platform, located in the Nice Cote d'Azur University to acquire second harmonic generation (SHG) images.

We used a LSM780NLO (Zeiss, Jena, Germany) coupled to a MaiTai HP Deepsee (Spectra Physics, Milpitas, CA) laser tuned at 880 nm. For detection, we used a GaAsP detector in reflexion to acquire simultaneously a 440-nm SHG signal and a 575- to 610-nm autofluorescence signal. We used 10×/0.3 objective for imaging. Collagen I is a well-known harmonophore, emitting SHG owing to its intrinsic molecular property and to its asymmetric scaffold of the collagen fibrils. Contrary to fluorescence, which has a tendency to bleach or fade, the SHG signal is stable over time, as long as collagen structure is not disturbed. Then, the SHG signal is a good signature of the collagen combining concentration and organization. The stronger the SHG signal, the greater the quantity or better was the fibers' orientation per pixel, which corresponds with an analysis volume of approximately 600 nm in diameter. For quantification, we developed dedicated scripts coded in MATLAB (The MathWorks, Natick, MA) using Bio-Formats libraries from OME[13] to import data. We quantified three-dimensional samples (1.3 × 1.3 × 0.4 mm), considering the total SHG intensity over the sample, the acquisition parameters being precisely constant. To estimate the score of fiber thickness and organization, we defined a blind protocol. The program showed images in random order to the operator. Based on visual impression, it defined both scores on a 0 (low) to 5 (high) scale.

Table 1. Subtypes of Collagen Fibers Among the Different Grafts Analyzed[2,7,14]

Graft	Type of Collagen Fibers
Tarsus	I, III, VI
Conchal cartilage	I, II
Sclera	I, III
Hard palate	I, III
Dermis	I, III

Assessment of the Best Posterior Lamella Graft to Replace the Tarsus

To determine which graft was the most appropriate to replace the tarsus, we summarized all the results in a table attributing 2 points to each biomechanical, histological, and optical properties. One point was attributed to the graft presenting 25% or less (double sided) of difference compared with the tarsus (0 point if the difference was >25%) for the continuous variables (Young's modulus, tensile strength, SHG signal, and fiber size) and 1 point for the graft belonging to the same category as the tarsus for categorical variables (elastin fibers repartition and subtype of collagen fibers based on the literature knowledge summarized in Table 1). For optical properties, we did not figure fiber orientation because it was already taken into consideration in SHG signal.

Statistical Analyses

Descriptive data were presented as mean (range) or median. Statistical analysis was performed by using the two-sided Student *t*-test with SPSS v25 (SPSS, Inc, Chicago, IL) software. A *P* value of less than 0.05 was considered statistically significant. All the grafts were compared with the tarsus. Therefore, a *P* value of less than 0.05 meant that the graft was statistically different from the tarsus. The higher the *P* value, the closer was the graft to the tarsus.

Results

Biomechanical Features

The biomechanical features of each graft are provided in Figure 2. The mean Young's Modulus was 8.92 MPa (range, 2.90–22.90 MPa), 1.05 MPa (range, 0.39–1.76 MPa), 8.72 MPa (range, 2.0–23.50 MPa), 2.57 MPa (range, 0.41–4.35 MPa), and 1.4 MPa (range, 0.71–2.30 MPa) for the tarsus, the conchal cartilage, the sclera, the hard palate mucosa, and the dermis, respectively. Statistical analysis found that the sclera

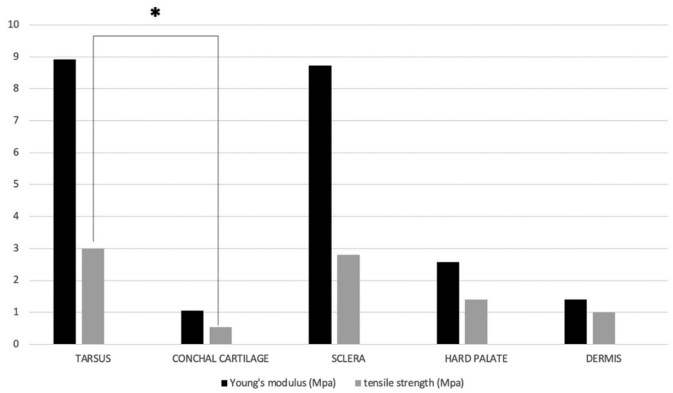

Figure 2. Biomechanical results. Young's modulus and tensile strength are presented for each graft. *Statistical difference compared with the tarsus (Student *t*-test).

was closest to the tarsus ($P = 0.97$), and conchal cartilage was furthest away ($P = 0.06$).

The mean tensile strength was 3.0 MPa (range, 1.70–6.88 MPa), 0.54 MPa (range, 0.13–0.79 MPa), 2.87 MPa (range, 1.23–5.40 MPa), 1.4 MPa (range, 0.21–2.40 MPa), and 1.0 MPa (range, 0.46–1.43 MPa) for the tarsus, the conchal cartilage, the sclera, the hard palate mucosa, and the dermis, respectively. Statistical analysis found that the sclera was closest to the tarsus ($P = 0.91$) and conchal cartilage was furthest away ($P = 0.03$).

Collagen and Elastin Fiber Analysis

The collagen fibers were predominant in all grafts. By contrast, wide variations of elastin fibers were found (Figs. 3 and 4). Verhoeff staining demonstrated that the conchal cartilage and the dermis had the most important ratio of elastin fibers (25%–50%), followed by the tarsus and the hard palate mucosa (1%–25%); the sclera did not exhibit elastin fibers in its composition (<1%).

Biphotonic Microscopic Assessment

SHG results are summarized in Figure 5. The median SHG intensity was 221 arbitrary units (a.u.)

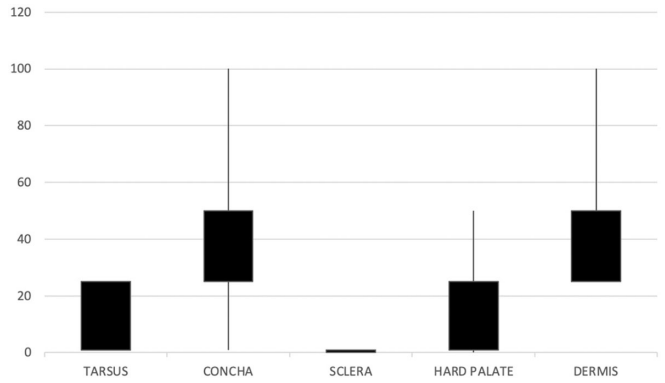

Figure 4. Proportion of elastin fibers/collagen fibers (%) for each graft.

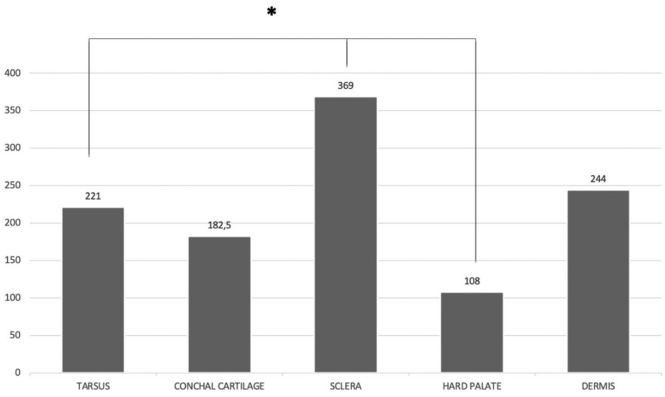

Figure 5. Median SHG intensity signal (arbitrary units) for each graft. *Statistical difference compared with the tarsus (Student *t*-test).

(range, 165–362 a.u.), 182 a.u. (range, 35–259 a.u.), 369 a.u. (range, 206–533 a.u.), 108 a.u. (range, 34–208 a.u.), and 244 a.u. (range, 195–388 a.u.) for the tarsus, the conchal cartilage, the sclera, the hard palate mucosa, and the dermis, respectively. Statistical analysis found that the dermis was closest to the tarsus ($P = 0.45$) and hard palate mucosa was furthest away ($P = 0.03$).

The mean fiber size and orientation are presented in Figures 6 and 7. The mean fibers' size calculated by using a scale ranging from 0 to 5 were 2.07 (range, 1–3), 2.69 (range, 1–4), 2.56 (range, 2–4), 1.60 (range,

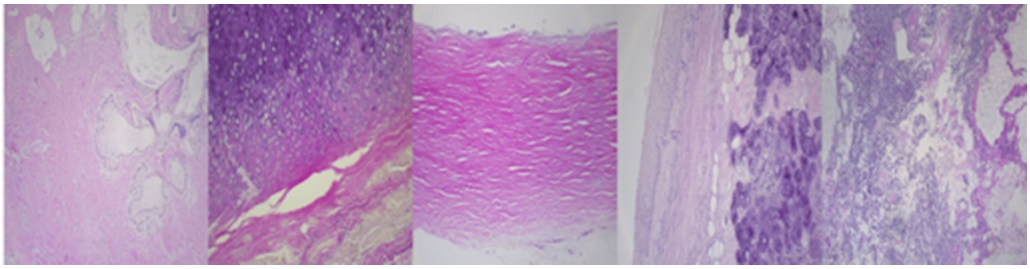

Figure 3. Verhoeff staining (original magnification ×50). The collagen fibers are colored in pink and the elastin fibers in purple. From left to right: tarsus, conchal cartilage, sclera, hard palate mucosa, and dermis.

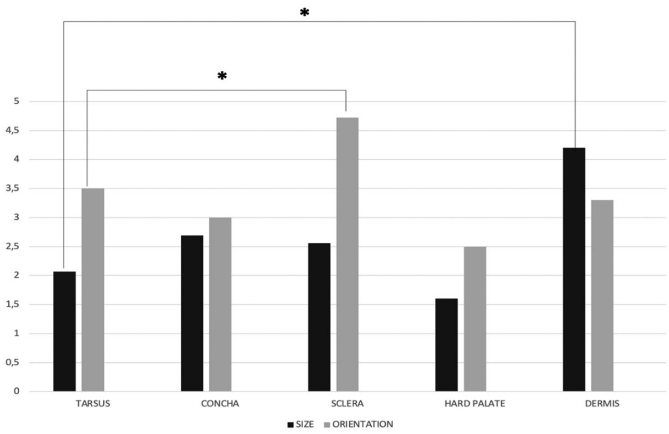

Figure 6. Mean size and orientation of collagen fibers assessed by biphotonic microscopy by using a scale ranging from 0 to 5. *Statistical difference compared with the tarsus (Student *t*-test).

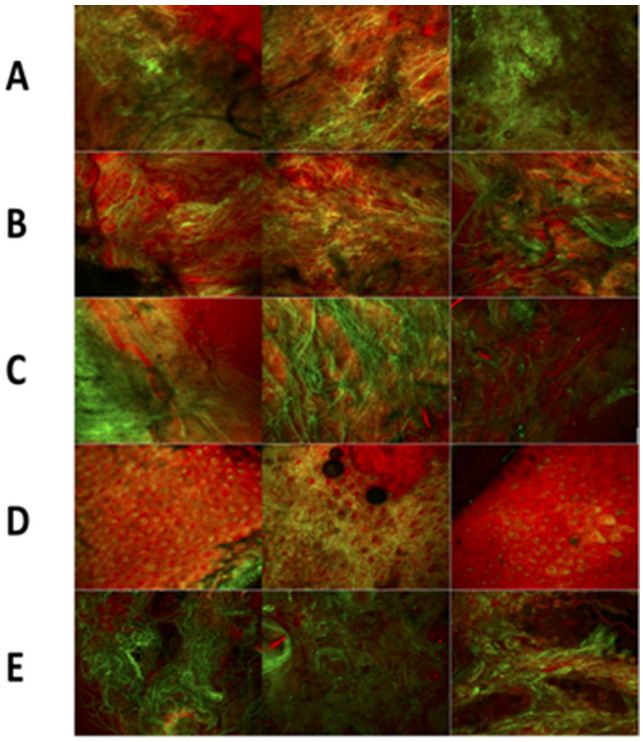

Figure 7. Examples of collagen fiber size and orientation assessed by biphotonic microscopy. Collagen fiber SHG signal is depicted in green. Tissue autofluorescence is depicted in red. (**A**) Tarsus. (**B**) Conchal cartilage. (**C**) Sclera. (**D**) Hard palate mucosa. (**E**) Dermis.

Table 2. The Most Suitable Graft to Replace the Tarsus

	Young's Modulus (MPa)	Tensile Strength (MPa)	Elastin Fibers (%)	Type of Collagen Fibers	SHG Intensity	Collagen Fibers Size	Total
Conchal cartilage	0	0	0	0	1	0	**1**
Sclera	1	1	0	1	0	0	**3**
Hard palate	0	0	1	1	0	1	**3**
Dermis	0	0	0	1	1	0	**2**

1–3), and 4.2 (range, 4–5) for the tarsus, the conchal cartilage, the sclera, the hard palate mucosa, and the dermis, respectively. Statistical analysis found that the hard palate was closest to the tarsus ($P = 0.09$) and the dermis was furthest away ($P < 0.001$).

The mean fibers orientation graded in a scale ranging from 0 to 5 were 3.5 (range, 1–5), 3.0 (range, 1–5), 4.7 (range, 3–5), 2.5 (range, 1–5), and 3.3 (range, 2–4) for the tarsus, the conchal cartilage, the sclera, the hard palate mucosa, and the dermis, respectively. Statistical analysis found that the dermis was closest to the tarsus ($P = 0.64$) and sclera was furthest away ($P = 0.04$).

Assessment of the Best Posterior Lamella Graft to Replace the Tarsus

Regarding the biomechanical properties, the sclera was the most suitable graft to replace the tarsus (Table 2). In terms of collagen and elastin fibers repartition, the hard palate mucosa was found to be the closest to the tarsus. By studying the optical properties, all the grafts except the sclera shared similarities with the tarsus. When cumulating the results by attributing 2 points for each characteristic (biomechanical, histological, and optical), the hard palate mucosa and the sclera appeared to be the most suitable grafts to replace the tarsus.

Discussion

Many studies have aimed to investigate the best posterior lamellar graft to reconstruct an eyelid.[15] There is still no consensus regarding the ideal posterior lamella spacer. Most studies are based on clinical findings.[15] More fundamental studies based on the biomechanical, optical, and histological properties of each graft are currently lacking. In this study, we postulated that the tarsus was the graft of reference and we aimed to compare four different grafts based on their intrinsic features. The sclera was found to share roughly the same biomechanical properties. Optical

properties determined by bi-photonic microscopy revealed that SHG signal of the dermis and conchal cartilages were close to the tarsus. Regarding the fibers' size, the hard palate mucosa was roughly close to those encountered in the tarsus. There is still no classification comparing the intrinsic characteristics of each graft. We arbitrarily allocated 2 points for each graft's characteristic (biomechanical, optical, and histological); taken together, our data suggest that the hard palate mucosa and the sclera are the most suitable grafts to replace the tarsus.

To our knowledge, this is the first ophthalmological study comparing the biomechanical, histological, and microscopic optical characteristics of five commonly used posterior lamella grafts. Comparing our results with the literature is challenging because of the different measurement methods used. The biomechanical features of a tissue can be assessed by indentation or traction methods. Indentation induces microscopic deformation at the point of contact, whereas traction involves the whole tissue. In our experience, traction is more suitable, which is in accordance with the study performed by McKee et al.[16] Usually, traction is associated with higher Young modulus values compared with indentation. This finding is explained by the fact that traction measures involve several proteins such as collagen, actin and even water in the calculation of Young modulus, which is not the case when performing indentation measurements. For example, we found a Young's Modulus of 8.92 MPa and 8.72 MPa for the tarsus and the sclera, respectively. Sun et al.[17] and Eilaghi et al.[18] found a Young's modulus of 1.73 MPa and 2.9 MPa for the tarsus and the sclera, respectively. These differences could be explained by the nature of the samples, which were harvested in frozen cadavers in our study, whereas they were freshly harvested in living patients in other studies. Furthermore, in our study, we collected perilimbic sclera, which is approximately 0.66 mm thick. In the study by Eilaghi et al., the authors collected sclera from the posterior pole, which is thicker and therefore probably more resistant than the perilimbic sclera. We found a Young's modulus of 1.05 MPa for the conchal cartilage, which is in accordance with previous studies conducted by Ernst et al. (1.14 MPa)[14] and Nimeskern et al. (1.87 MPa).[19] In our study, the elastin fiber distribution was almost similar in the hard palate and the tarsus, which is consistent with the results provided by Ciano and Beatty.[20] We found that elastin fibers were over-represented in the dermis (Fig. 3). This finding could be explained by the fact that we harvested the dermis in the preauricular area where an actinic elastosis may frequently occur.[21] We did not find other studies comparing the SHG signal of posterior lamella grafts.

Our results suggest using the hard palate mucosa or sclera for reconstructing posterior lamella defects. The clinical advantages and disadvantages of the different posterior lamellar grafts are provided in Table 3 and should also be taken into consideration. In contrast with the United States, donor sclera banks do not exist in France limiting our experience with this graft. Several studies found favorable results when wrapping orbital implants in donor sclera without significant implant exposure.[22,23] The literature regarding the donor sclera for the eyelid reconstruction or lid lengthening is scarce and no conclusion can be drawn. Nonetheless, Kamiya and Kitajima.[24] showed in a study of five patients that preserved sclera grafts were as effective as auricular cartilage grafts in terms of functional and aesthetic eyelid outcomes.

Our study presents several limitations. First, our study suffers from a small sample size and a large age distribution. Age is known to alter the resistance of a tissue. However, in this study, each patient was their her own control, thus limiting this bias. Second, all samples were harvested in a full-thickness fashion and cut into 10-mm-wide pieces. It is likely that manipulation of the grafts may result in significant intrinsic tissue changes. In addition, all our samples provided from fresh frozen cadavers (1–15 days) and not from living patients. Interestingly, Huang et al.[25] showed that cadaveric tendons frozen-thawed less than three cycles harbored

Table 3. Clinical Advantages and Disadvantages of Each Posterior Lamella Graft

	Mucosal Surface	Available in Large Amount	Easy to Harvest	Low Donor Site Morbidity	Low Price	Risk of Disease Transmission
Tarsus	+	−	+	+	+	−
Concha	−	−	+	+	+	_
Donor sclera	−	+	+	+	_	+
Hard palate	+	+	−	−	+	_
Dermis	−	+	+	+	+	_

a similar Young modulus compared with fresh samples. Although tendons have a different microanatomy from the tarsal plate, both are composed primarily of collagen fibers. Third, we could not use SHG signal to analyze the elastin fibers. Elastin is known to influence the properties of cartilage. Nimeskern et al.[26] demonstrated that the mechanical properties were more related to elastin in ear cartilage, whereas they were more related to the collagen fibers in the articular cartilage. Fourth, we did not investigate aggrecan, cartilage oligomeric matrix proteins, and glycosaminoglycans, which play a role in the stiffness and resistance of the tissues.[2] These molecules could explain why the Young's modulus was incredibly weak in the hard palate mucosa, despite sharing almost the same SHG signal and collagen fiber orientation than the tarsus. Finally, our study design did not allow us to investigate graft shrinkage. Graft shrinkage is probably the most meaningful clinical feature to consider when reconstructing a posterior lamella eyelid defect. Only one clinical study found that the hard palate mucosa had a lower retraction rate compared with acellular dermis grafts.[27]

Conclusions

There is no ideal posterior lamella graft to replace the tarsus. Although not fully applicable in clinical practice, our preliminary results suggest that the hard palate mucosa ant the sclera are the most appropriate posterior lamella grafts. Further clinical studies focused on graft shrinkage with long follow-up are needed to confirm our preliminary results.

Acknowledgments

Disclosure: **K. Martini**, None; **S. Schaub**, None; **C. Bertoloto**, None; **S. Baillif**, None; **S. Lassalle**, None; **P. Martel**, None; **A. Martel**, None

References

1. Martel A, Farah E, Zmuda M, Almairac F, Jacomet PV, Galatoire O. Autologous dermis graft versus conchal cartilage graft for managing lower eyelid retraction: A comparative study. *Eur J Ophthalmol*. 2021;31:1733–1740. Published online June 12, 2020:112067212093440, doi:10.1177/1120672120934408.
2. Milz S, Neufang J, Higashiyama I, Putz R, Benjamin M. An immunohistochemical study of the extracellular matrix of the tarsal plate in the upper eyelid in human beings. *J Anat*. 2005;206(1):37–45, doi:10.1111/j.0021-8782.2005.00363.x.
3. Pieh S, Kuchar A, Novak P, Kunstfeld R, Nagel G, Steinkogler FJ. Long term results after surgical basal cell carcinoma excision in the eyelid region. *Br J Ophthalmol*. 1999;83(1):85–88.
4. Margo CE, Waltz K. Basal cell carcinoma of the eyelid and periocular skin. *Surv Ophthalmol*. 1993;38(2):169–192.
5. Hishmi AM, Koch KR, Matthaei M, Bölke E, Cursiefen C, Heindl LM. Modified Hughes procedure for reconstruction of large full-thickness lower eyelid defects following tumor resection. *Eur J Med Res*. 2016;21(1):1–8.
6. Stephenson CM, Brown BZ. The use of tarsus as a free autogenous graft in eyelid surgery. *Ophthal Plast Reconstr Surg*. 1985;1(1):43–50.
7. Ito R, Fujiwara M, Nagasako R. Hard palate mucoperiosteal graft for posterior lamellar reconstruction of the upper eyelid: histologic rationale. *J Craniofac Surg*. 2007;18(3):7.
8. Wearne MJ. Autogenous hard palate mucosa: the ideal lower eyelid spacer? *Br J Ophthalmol*. 2001;85(10):1183–1187, doi:10.1136/bjo.85.10.1183.
9. Bartley GB, Kay PP. Posterior lamellar eyelid reconstruction with a hard palate mucosal graft. *Am J Ophthalmol*. 1989;107(6):609–612, doi:10.1016/0002-9394(89)90257-2.
10. Chen J, Ahmad R, Li W, Swain M, Li Q. Biomechanics of oral mucosa. *J R Soc Interface*. 2015;12(109):20150325, doi:10.1098/rsif.2015.0325.
11. Parodi PC, Calligaris F, De Biasio F, De Maglio G, Miani F, Zeppieri M. Lower lid reconstruction utilizing auricular conchal chondral-perichondral tissue in patients with neoplastic lesions. *BioMed Res Int*. 2013;2013:837536.
12. Matsuo K, Hirose T, Takahashi N, Iwasawa M, Satoh R. Lower eyelid reconstruction with a conchal cartilage graft. *Plast Reconstr Surg*. 1987;80(4):547–552.
13. Linkert M, Rueden CT, Allan C, et al. Metadata matters: access to image data in the real world. *J Cell Biol*. 2010;189(5):777–782.
14. Bos EJ, Pluemeekers M, Helder M, et al. Structural and mechanical comparison of human ear, alar, and septal cartilage. *Plast Reconstr Surg Glob Open*. 2018;6(1):e1610, doi:10.1097/GOX.0000000000001610.

15. Oestreicher JH, Pang NK, Liao W. Treatment of lower eyelid retraction by retractor release and posterior lamellar grafting: an analysis of 659 eyelids in 400 patients. *Ophthal Plast Reconstr Surg*. 2008;24(3):207–212.
16. McKee CT, Last JA, Russell P, Murphy CJ. Indentation versus tensile measurements of Young's modulus for soft biological tissues. *Tissue Eng Part B Rev*. 2011;17(3):155–164, doi:10.1089/ten.teb.2010.0520.
17. Sun MT, Pham DT, O'Connor AJ, et al. The biomechanics of eyelid tarsus tissue. *J Biomech*. 2015;48(12):3455–3459, doi:10.1016/j.jbiomech.2015.05.037.
18. Eilaghi A, Flanagan JG, Tertinegg I, Simmons CA, Wayne Brodland G, Ross Ethier C. Biaxial mechanical testing of human sclera. *J Biomech*. 2010;43(9):1696–1701, doi:10.1016/j.jbiomech.2010.02.031.
19. Nimeskern L, Pleumeekers MM, Pawson DJ, et al. Mechanical and biochemical mapping of human auricular cartilage for reliable assessment of tissue-engineered constructs. *J Biomech*. 2015;48(10):1721–1729, doi:10.1016/j.jbiomech.2015.05.019.
20. Ciano J, Beatty BL. Regional quantitative histological variations in human oral mucosa: quantitative variations in human oral mucosa. *Anat Rec*. 2015;298(3):562–578, doi:10.1002/ar.23097.
21. Bouissou H, Pieraggi MT, Julian M, Savait T. The elastic tissue of the skin: a comparison of spontaneous and actinic (solar) aging. *Int J Dermatol*. 1988;27(5):327–335.
22. Jongman HP, Marinkovic M, Notting I, et al. Donor sclera-wrapped acrylic orbital implants following enucleation: experience in 179 patients in the Netherlands. *Acta Ophthalmol (Copenh)*. 2016;94(3):253–256.
23. Custer PL, McCaffery S. Complications of sclera-covered enucleation implants. *Ophthal Plast Reconstr Surg*. 2006;22(4):269–273.
24. Kamiya H, Kitajima Y. Successful use of preserved sclera of eyelid reconstruction. *Eur J Dermatol*. 2003;13(3):267–271.
25. Huang H, Zhang J, Sun K, Zhang X, Tian S. Effects of repetitive multiple freeze–thaw cycles on the biomechanical properties of human flexor digitorum superficialis and flexor pollicis longus tendons. *Clin Biomech*. 2011;26(4):419–423.
26. Nimeskern L, Utomo L, Lehtoviita I, et al. Tissue composition regulates distinct viscoelastic responses in auricular and articular cartilage. *J Biomech*. 2016;49(3):344–352, doi:10.1016/j.jbiomech.2015.12.032.
27. Sullivan SA, Dailey RA. Graft contraction: a comparison of acellular dermis versus hard palate mucosa in lower eyelid surgery. *Ophthal Plast Reconstr Surg*. 2003;19(1):14–24.